Pergamon

0196-8904(95)00215-4

Energy Convers. Mgmt Vol. 37, No. 5, pp. 505–520, 1996

0196-8904/96 $15.00 + 0.00

MODELING OF NATURAL TURBULENT FLOW IN A PASSIVELY HEATED ZONE

SEYHAN UYGUR and NILÜFER EĞRİCAN

Mechanical Engineering Department, Istanbul Technical University, 80191 Gümüşsuyu, Istanbul, Turkey

(Received 2 March 1995; received for publication 11 July 1995)

Abstract—In the present study, a modified turbulence model has been developed having the goals of representing the dominant buoyancy effect, and also the low turbulence due to buoyancy and the viscous effects in the vicinity of the wall for a zone heated passively with a Trombe wall, where the magnitudes of aspect ratio and Rayleigh number equal to one and 10^{10}, respectively. Standard viscosity/diffusivity and Daly Harlow approximations for the definition of the scalar quantities are used and compared to each other. The model and the code solving the governing equations may be applied to similar structures, namely, enclosures with aspect ratio about one, having inlet and outlet openings on the heated side. Also, improving the computational convergence and decreasing the computer time are goals of this work.

Turbulence model Trombe wall Natural convection

NOMENCLATURE

A = Aspect ratio
a_i = Coefficients of discretized equation [equation (16)]
$c_{\epsilon 1}, c_{\epsilon 2}, c_{\epsilon 3}$ = Coefficients of turbulence model [equation (8)]
c_ϕ = Coefficient of modified turbulence model [equation (13)]
d = Distance between glass plate and Trombe wall (m)
D = Source term in turbulence model [equation (7)]
E = Source term in turbulence model [equation (8)]
f_1, f_2, f_μ = Functions of turbulence model [equation (8)]
g_i = Gravitational acceleration (m/s^2)
G_k = Buoyancy production/destruction (m^2/s^3)
H = Height of enclosure (m)
k = Turbulence kinetic energy (m^2/s^2)
L = Width of enclosure (m)
n = Number of iteration or normal direction
P_k = Shear stress production (m^2/s^3)
P = Pressure (Pa)
Ra = Rayleigh number
Re_t = Turbulence Reynolds number
s = Width of ventilation hole (m)
S_ϕ^ϕ = Dependent source term
S_U^ϕ = Independent source term
T = Temperature (°C)
t = Time (s)
u_i = Fluctuative velocity (m/s)
U = Horizontal velocity (m/s)
U_i = Velocity (m/s)
V = Vertical velocity (m/s)
w = Thickness of Trombe wall (m)
x = Horizontal coordinate
y = Vertical coordinate

Greek symbols

α = Under relaxation factor
β = Volume expansivity (1/K)
ϵ = Dissipation of turbulence kinetic energy (m^2/s^3)
ϕ = Scalar dependent variable
ϕ_i = Any dependent variable in numerical solution [equation (16)]
Λ = Shear stress production or buoyancy production/destruction or turbulent viscosity or density [equation (20)]

μ = Dynamic viscosity (kg/ms)
μ_t = Turbulent dynamic viscosity (kg/ms)
ν = Kinematic viscosity (m^2/s)
ν_t = Turbulent kinematic viscosity (m^2/s)
ρ = Density (kg/m^3)
$\sigma_k, \sigma_t, \sigma_\varepsilon$ = Prandtl numbers for turbulence kinetic energy, temperature and dissipation of turbulence kinetic energy, respectively

Subscript

in = Inlet value

1. INTRODUCTION

Natural convection in square and tall enclosures has a wide theoretical background in the literature [1–3]. Since the problem is related to general events in energy conversion and daily life, namely nuclear reactors, electronic coolings and residential zones, also experimental studies, including the scope of modeling convection in enclosures, have been growing aspects of heat transfer [4, 5]. In the past decade, the turbulent characteristics of this type of flow have been the major part of the investigations. Both numerical and experimental results have been obtained in tall enclosures [6, 7] and square ones [8, 9] in modeling the flow. Especially, the control of indoor air has increased interest also in non-buoyant turbulent air flow due to cooling and ventilation [10–15]. However, these experiments and numerical calculations are focused on forced convection, namely the inertia driven flow, not the natural one.

Beyond a critical Rayleigh number, buoyancy driven flow in enclosures has turbulent characteristics, depending on the aspect ratio. The core effect on the boundary layers and the dominant buoyancy force disable an exact solution for such a flow.

The enclosure modeled in this study represents a zone heated by means of solar radiation (Fig. 1). The system is called the "passive system with a Trombe wall" [16]. The solar radiation is absorbed by the glass plate, usually a double glazed one, installed on the south face of the zone. The wall, named "Trombe wall", has been constructed just behind the glass plate. The zone is heated via conduction heat transfer through the Trombe wall and convection through the ventilation holes on it. Thus, the zone may be considered as an enclosure having two openings on the same side, where the magnitudes of the aspect ratio and Rayleigh number are one and 2×10^{10}–6×10^{10}, respectively. The upper opening is the hot air inlet and the lower one is the outlet of the air flow cooled in the enclosure. Turbulence is either produced or destructed inside the zone, depending on the dominant buoyancy force, temperature stratification and the wall effect. A detailed definition of this mechanism is present in Refs [17, 18].

Since viscous effects are dominant somewhere in the zone due to the low level of turbulence, there is a lack of appropriate turbulent model in the literature for such a system. Most of the turbulence models developed in the past were for the solution of isothermal forced flows. Developments in modeling the natural turbulent convection have also been accelerated, as environmental aspects, such as diffusion of pollutants, have been popular in the last decade [19–22]. The attempt to solve

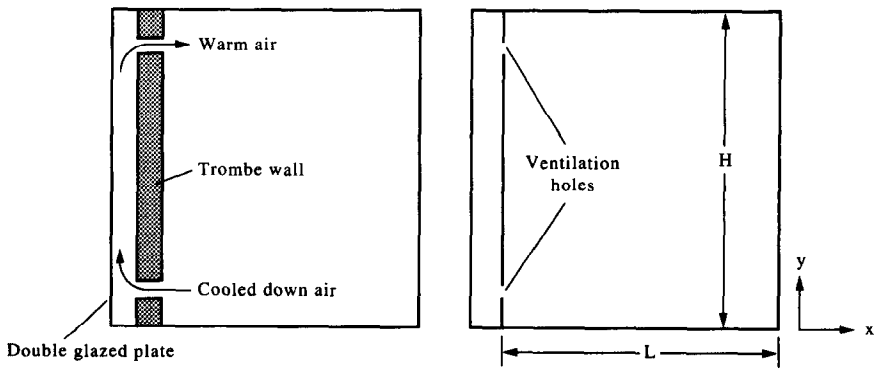

Fig. 1. Schematic diagram of the passive system heated by means of the Trombe wall.

the flows which have low Reynolds number begins with Ref. [23], which is followed with several ones [24]. Reviews of the models in the vicinity of the wall and for the case of low Reynolds number flows are present in Refs [20] and [21].

Unfortunately, these models are not universal, and it is almost decided that a turbulence model should be problem dependent and valid for only similar cases [22].

In the present study, a modified turbulence model has been developed to solve the natural convective flow in a zone heated passively with a Trombe wall. The model and the code solving the governing equations may be applied to similar structures. Another goal of this work is to improve the computational convergence and decrease the computer time.

2. FORMULATION

The continuity, momentum, and energy equations governing the flow in this geometry are, respectively:

$$\rho \frac{\partial (U_i)}{\partial x_i} = 0 \tag{1}$$

$$\rho \left(\frac{\partial U_i}{\partial t} + U_j \frac{\partial U_I}{\partial x_J} \right) = \frac{\partial}{\partial x_J} \left[\mu \frac{\partial U_i}{\partial x_J} - \rho \overline{u_i u_j} \right] - \frac{\partial P}{\partial x_i} + \rho g_i \tag{2}$$

$$\rho \left(\frac{\partial T}{\partial t} + U_j \frac{\partial T}{\partial x_J} \right) = \frac{\partial}{\partial x_I} \left[\frac{\mu}{\mathrm{Pr}} \frac{\partial T}{\partial x_I} - \rho \overline{u_i T'} \right]. \tag{3}$$

Importing the Boussinessq approximation, the body force appearing in equation (2) is represented by buoyancy.

According to the eddy viscosity and eddy diffusivity approximations [22], the Reynolds stresses and turbulent heat fluxes are defined as:

$$-\overline{u_i u_j} = \nu_t \left(\frac{\partial U_i}{\partial x_j} + \frac{\partial U_j}{\partial x_i} \right) - \tfrac{2}{3} k \delta_{ij} \tag{4}$$

$$-\overline{u_i T'} = \frac{\nu_t}{\sigma_t} \frac{\partial T}{\partial x_i} \tag{5}$$

where

$$\nu_t = f_\mu c_\mu \frac{k^2}{\epsilon}. \tag{6}$$

3. TURBULENCE MODEL

The origin of the modified model is the k-ϵ one [22]. In this model, the differential equations for the turbulent kinetic energy and the dissipation of this energy in general indices form are:

$$\rho \frac{Dk}{Dt} = \frac{\partial}{\partial x_i} \left[\left(\frac{\mu_t}{\sigma_k} + \mu \right) \frac{\partial k}{\partial x_i} \right] + \rho P_k + \rho G_k - \rho \epsilon + \rho D \tag{7}$$

$$\rho \frac{D\epsilon}{Dt} = \frac{\partial}{\partial x_i} \left[\left(\frac{\mu_t}{\sigma_\epsilon} + \mu \right) \frac{\partial \epsilon}{\partial x_i} \right] + f_1 c_{\epsilon 1} \frac{\epsilon}{k} \rho (P_k + c_{\epsilon 3} G_k) - f_2 c_{\epsilon 2} \rho \frac{\epsilon^2}{k} + \rho E \tag{8}$$

where P_k is the shear stress production,

$$P_k = -\overline{u_i u_j} \frac{\partial U_i}{\partial x_j} \tag{9}$$

and G_k is the buoyancy production term,

$$G_k = -g_i \beta \overline{u_i T'}. \tag{10}$$

The source terms, D and E, where

$$D = -2\nu\left(\frac{\partial k^{1/2}}{\partial x_j}\right)^2 \tag{11}$$

$$E = -2\mu\mu_t\left(\frac{\partial^2 U_i}{\partial x_j \partial x_l}\right)^2 \tag{12}$$

are added to use the Dirichlet boundary condition for dissipation of the turbulent kinetic energy for computational reasons [24]. In this study, they are not included due to the justifications below:

(i) In the case of using D, instead of the equation for the dissipation of kinetic energy itself, the differential equation for the dissipation variable $\tilde{\epsilon} = \epsilon + D$ is solved [24]. It sounds more physical to solve the differential equation for the dissipation of kinetic energy rather than the one for the dissipation variable. The computational advantage of using the Dirichlet boundary condition is compensated by the model developed here; and the gradient of dissipation is taken as zero.

(ii) The source term E is included by the authors of Ref. [24] to represent the change of dissipation with respect to the distance to the wall. In the case of importing E, this change accelerates more than that of the kinetic energy of turbulence. Thus, the source term depends on grid dimensions strongly.

A wide discussion on these terms is present in Ref. [18]. Boundary conditions, coefficients, and the constants used in the modified model developed here are summarized in Table 1.

The function f_μ representing the effect of molecular viscosity on shear stress does not depend on the grid dimension and location. In low Reynolds number k-ϵ turbulent models, the function f_1 is used in order to decrease the kinetic energy of turbulence in the vicinity of the wall by increasing the dissipation. However, this duty is held by the function f_μ. So, in this model, the function f_1 is taken as unity. The function f_2, on the other hand, consists of the effect of low Reynolds number on the destruction term in the dissipation equation [equation (8)]; and it is imported from the Jones and Launder's model [23].

The characteristics of the new model, including the modifications defined above, will be called the "standard approximation" further in the text because the flux definitions have been used by means of the eddy viscosity/diffusivity approximation [equations (5) and (6)]. Otherwise, instead of the standard turbulent flux approximation, the Daly Harlow approximation [25] is used for the definition of the fluctuation part of the temperature.

Thus, the turbulent component of temperature is defined also in terms of velocity gradients:

$$-\overline{u_i\phi} = c_\phi \frac{k}{\epsilon} \overline{u_i u_k} \frac{\partial \phi}{\partial x_k}. \tag{13}$$

Here, c_ϕ is called the Daly Harlow constant. To make this coefficient compatible with the eddy diffusivity approximation, it is taken as equal to 3/2 of c_μ/σ_ϕ.

This new definition is imported into the buoyancy production/destruction term and energy equation. Thus, the following definitions are obtained for the buoyancy production/destruction term and the diffusion term of the energy equation:

$$G_k = -\frac{3}{2} g_i \beta \frac{c_\mu}{\sigma_\phi} \frac{k}{\epsilon} \nu_t \left(\frac{\partial U_i}{\partial x_j} + \frac{\partial U_j}{\partial x_i}\right) \frac{\partial T}{\partial x_k} \tag{14}$$

Table 1. Coefficients, functions and boundary conditions of the modified model

c_μ	$c_{\epsilon 1}$	$c_{\epsilon 2}$	$c_{\epsilon 3}$	σ_k	σ_ϵ	σ_t	σS_c
0.9	1.44	1.92	2.0	1.0	1.3	0.9	0.6
f_μ	f_1	f_2		ϵ_{wall}	k_{wall}		Re_t
$e^{-3.4/(1+Re_t^2)}$	1.0	$1.0 - 0.3e^{-Re_t^2}$		$\left.\frac{\partial \epsilon}{\partial x}\right\|_{wall} = 0.0$	$k_{wall} = 0.0$		$\rho\frac{k^2}{\mu\epsilon}$

Table 2. Variable dependent and independent source terms of the governing equations imported in this study

ϕ	S_U/Volume	S_P/Volume
U_i	$-\frac{\partial P}{\partial x_i}+(\mu+\mu_t)\frac{\partial^2 U_i}{\partial x_i^2}+(\mu+\mu_t)\frac{\partial^2 U_j}{\partial x_i \partial x_j}+\frac{\rho^{n-1}U_i^{n-1}}{\partial t}$	$-\frac{\rho^{n-1}}{\partial t}$
k	$\rho(P_k+G_k)+\frac{\rho^{n-1}k^{n-1}}{\partial t}$	$-c_\mu f_\mu \frac{\rho^2 k}{\mu_t}\frac{\rho^{n-1}}{\partial t}$
ϵ	$c_{\epsilon 1}f_1 c_\mu f_\mu \rho k \frac{P_k}{\mu_t}+c_{\epsilon 1}f_1 c_{\epsilon 3}\rho G_k \frac{\epsilon}{k}+\frac{\rho^{n-1}\epsilon^{n-1}}{\partial t}$	$-c_{\epsilon 2}f_2 c_\mu f_\mu \frac{\rho^2 k}{\mu_t}\frac{\rho^{n-1}}{\partial t}$
T	$\mathrm{Diff_T}=\frac{\partial}{\partial x_i}\left(\frac{\mu}{\mathrm{Pr}}\frac{\partial T}{\partial x_i}-2c_t\mu_t\frac{k}{\epsilon}\frac{\partial u_i}{\partial x_i}\frac{\partial T}{\partial x_i}+\frac{2}{3}c_t\rho\frac{k^2}{\epsilon}\frac{\partial T}{\partial x_i}\right)+\frac{\rho^{n-1}T^{n-1}}{\partial t}$	$-\frac{\rho^{n-1}}{\partial t}$

$$\mathrm{Diff_T}=\frac{\partial}{\partial x_i}\left(\frac{\mu}{\mathrm{Pr}}\frac{\partial T}{\partial x_i}-2c_\phi\mu_t\frac{k}{\epsilon}\frac{\partial U_i}{\partial x_i}\frac{\partial T}{\partial x_i}+\frac{2}{3}c_\phi\rho\frac{k^2}{\epsilon}\frac{\partial T}{\partial x_i}\right). \tag{15}$$

The rest of the additional terms in the energy equation due to this approximation are added to the source terms (Table 2).

4. NUMERICAL PROCEDURE

The numerical solution consists of discretization by a finite difference method [26] and an iterative solution included by the code developed in this study. The general form of the discretized differential equations is:

$$a_P^\phi \phi_P = \Sigma a_i^\phi \phi_i + S_U^\phi \tag{16}$$

where

$$a_P^\phi = \Sigma a_i^\phi - S_P^\phi. \tag{17}$$

The variable independent and dependent source terms, S_U and S_P, of the governing equations are listed in Table 2, and the grid distribution is illustrated in Fig. 2. The staggered grids, namely, the vectorial dependent variables and the scalar ones being inserted on the control volumes and the grid points, respectively [26], are generated in such a way that the dimensions of the control volumes are very tiny near the walls and become coarser towards the core region. In the code, the PLDS, power law differencing scheme for the convection terms, and SIMPLE, semi-implicit pressure linkage method for the pressure correction have been used.

The dependent variables are under relaxed according to the following three assumptions. For U, V, k, ϵ, T and C:

$$\frac{a_P^\phi}{\alpha}\phi_P = \Sigma a_i^\phi + S_U^\phi + \frac{1-\alpha}{\alpha}a_P^\phi \phi_P^{n-1} \tag{18}$$

for pressure;

$$P = P^* + \alpha_P P' \tag{19}$$

for stress production, buoyancy production, turbulent viscosity and density;

$$\Lambda = \Lambda^{n-1} + \alpha(\Lambda^n - \Lambda^{n-1}). \tag{20}$$

In equation (19), P^* and P' are, respectively, the incorrected and corrected pressures.

After trying a series of values for the under relaxation factors, it is agreed on the values listed in Table 3 to realize optimum convergence and computer time.

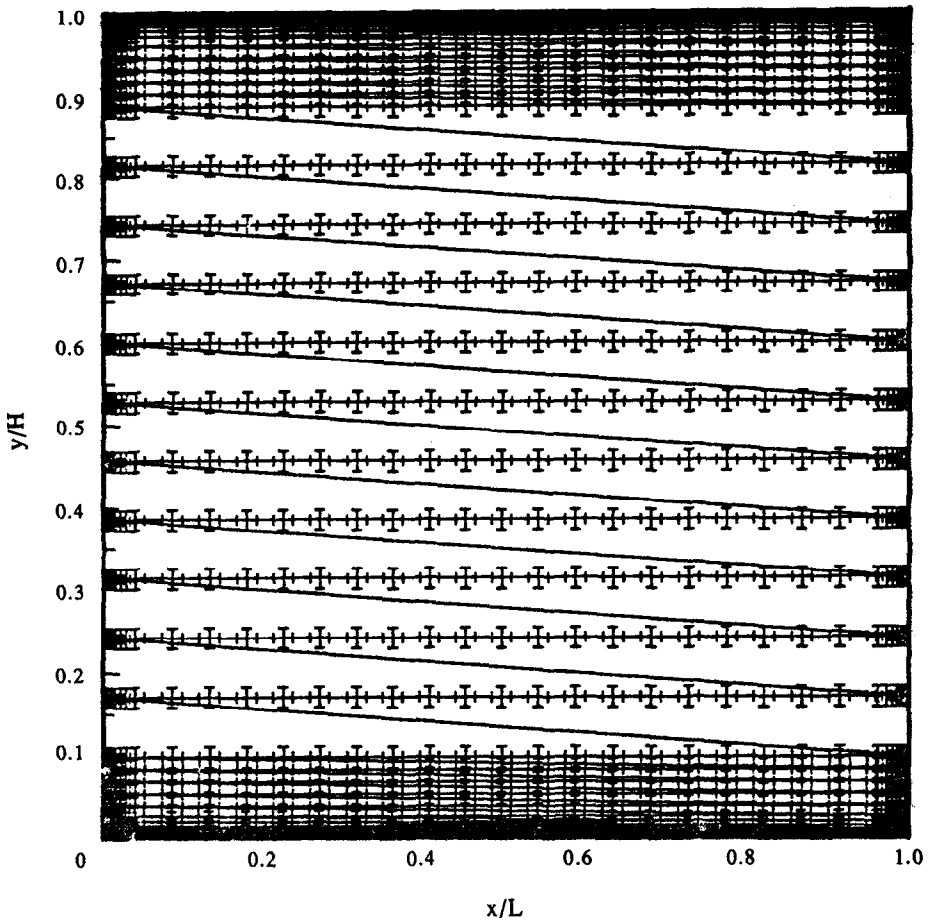

Fig. 2. Grid distribution inside the enclosure under investigation.

Table 3. Under relaxation factors imported in the study for optimum convergence and computer time for two-dimensional case

U	V	P	k	ϵ	T	P_k	G_k	μ_t	ρ
0.5	0.5	0.6	0.5	0.5	0.8	0.8	1.0	1.0	1.0

5. APPLICATION

The modified model has been applied to the flows studied widely in the literature. Figures 3 and 4 illustrate, respectively, the turbulent kinetic energy change along the enclosure width in a tall enclosure and in the vicinity of the wall. The results from past solutions have been compared with the ones obtained in this study, and it is concluded that the model is valid for tall enclosures.

The procedure of the general calculation of the convective flow in a zone heated with a Trombe wall consists of the following steps:

(i) Evaluation of the meteorological data for the location of the passively heated zone to obtain the radiation amounts and temperature values on the double glazed plate.
(ii) Prediction of the turbulent flow field in the gap between the double glazed plate and the Trombe wall.
(iii) Modeling the flow in the Trombe wall, which is made of a porous material, by means of the governing equations of laminar flow combined with Darcy's Law [27].
(iv) Executing the main part of the work by solving the modified turbulence model to predict the velocity and temperature fields inside the zone by means of both the standard and Daly Harlow approximations.

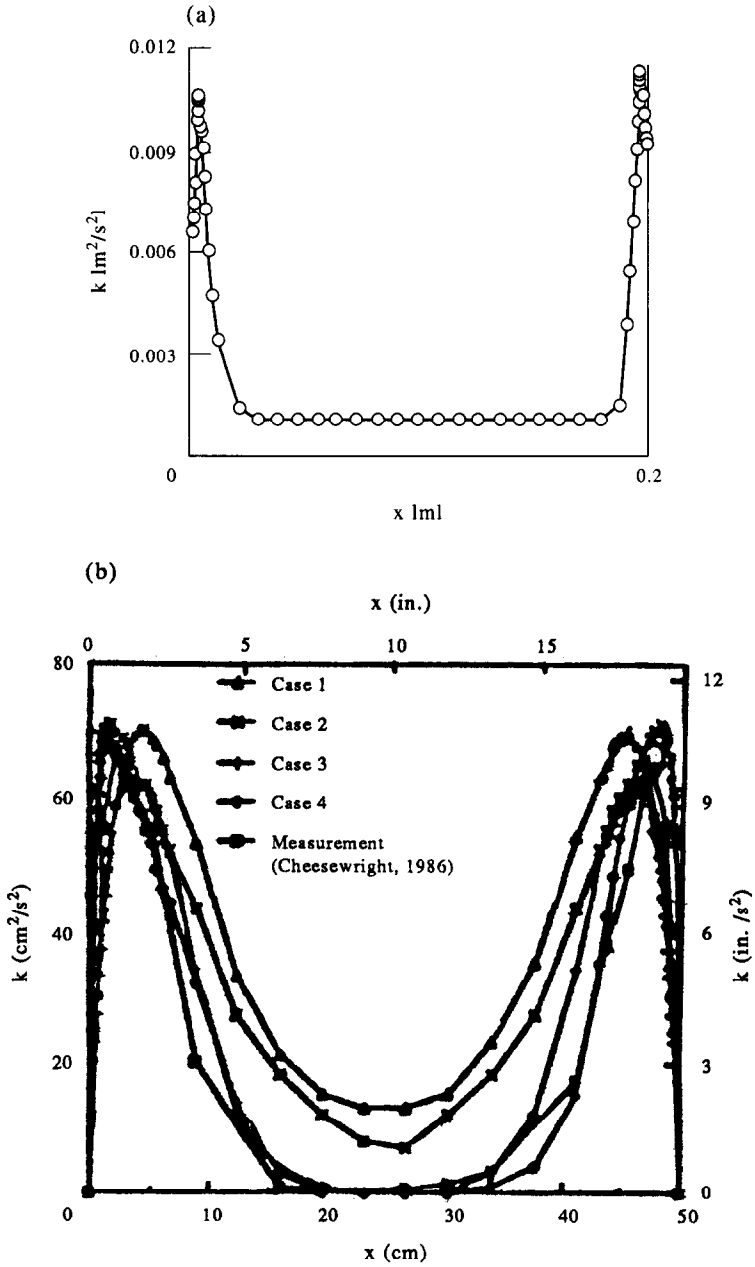

Fig. 3. Change of turbulent kinetic energy along the enclosure width in a tall enclosure: (a) result of the model developed in this study; (b) results of the models in literature [19].

In the third step, the natural convective flow field inside the porous Trombe wall is solved by the developed code, canceling the terms related to turbulence. The governing equations are given in Ref. [27], and its application in the present study is summarized in the Appendix.

Boundary conditions of the flow inside the zone are:

Vertical walls

$U_i = 0, \quad T = \text{const.},$
$k = 0, \quad \partial\epsilon/\partial y = 0.$

Horizontal walls

$U_i = 0, \quad \partial T/\partial x = 0,$
$k = 0, \quad \partial\epsilon/\partial x = 0.$

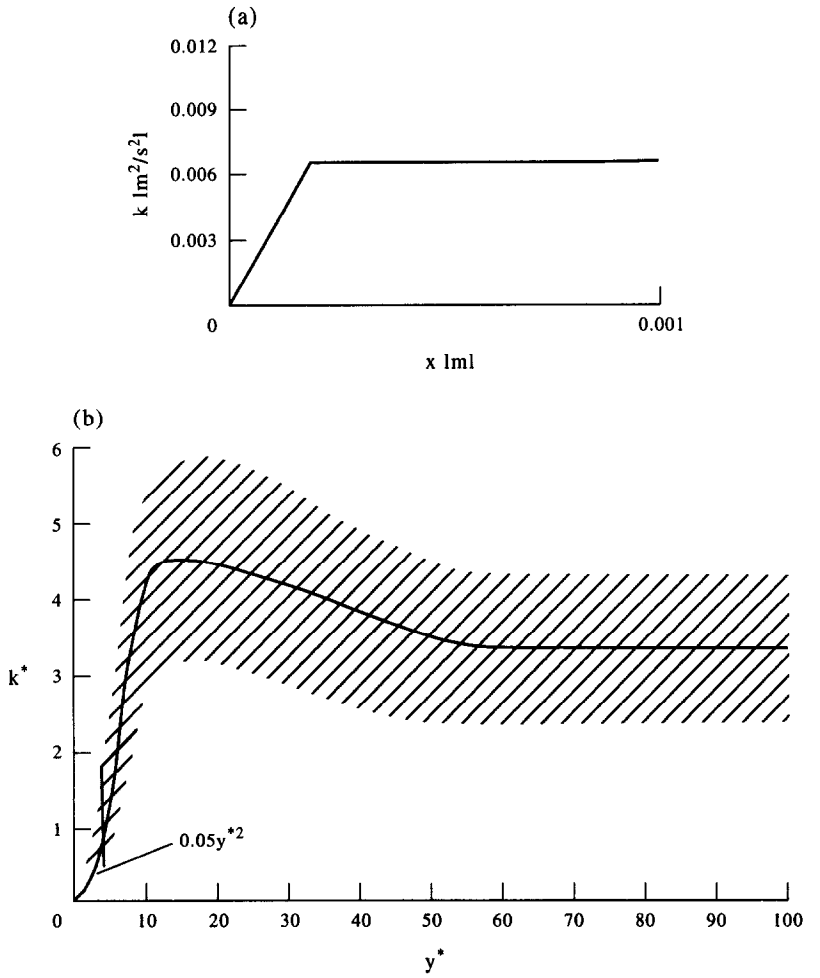

Fig. 4. Change of turbulent kinetic energy in the vicinity of the wall: (a) result of the model developed in this study; (b) results of the models in literature [20].

Upper opening, i.e. air inlet

$U_i = U_{in}$; $T = T_{in}$;
$k_{in} = 1.5x(0.04xU_{in})^2$
$\epsilon_{in} = k_{in}^{1.5}/(s/10)$.

At lower opening, i.e. air outlet, gradients of all dependent variables are constant.

6. RESULTS AND DISCUSSION

Both the standard and the Daly Harlow approximations of the model have been applied to the enclosures and they have been compared. Since the Daly Harlow approximation assumed in the modified model developed here consists of the non-isotropy of only the scalar quantities and non-isotropy of the velocity fluctuations is more important than that of the scalar ones in a tall enclosure, no difference has been found between the two approximations for a tall enclosure investigation. However, for a square enclosure, for the passively heated zone illustrated in Fig. 1, the Daly Harlow approximation represents the secondary flows at the lower cold corner and the unstable stratification better than the standard one (Figs 5 and 6). For the turbulent flows in which the buoyancy force is dominant, as in a passively heated zone, non-isotropy of the temperature fluctuations affects the flow field too much.

Especially, the secondary flows between the inlet air stream and the ceiling cause a greater difference between the two approximations near the ceiling [Fig. 7(a)]. Also, near the floor, due to

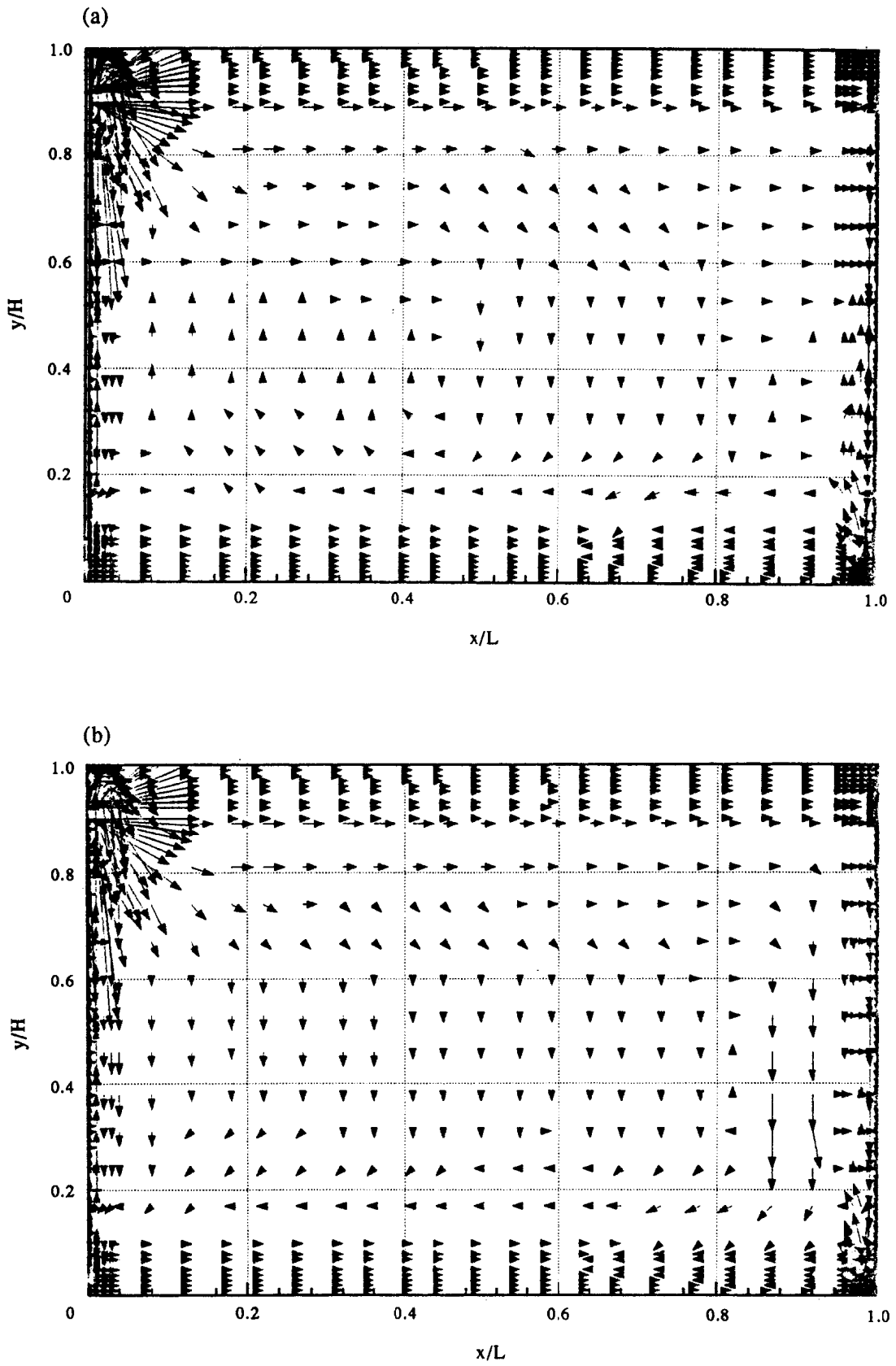

Fig. 5. Velocity vectors in the passively heated zone with a Trombe wall: (a) standard approximation; (b) Daly Harlow approximation.

the fluid outlet and the secondary flows at the lower cold corner, a great difference appears between the Daly Harlow and standard approximations [Fig. 7(b)]. Because turbulence is very low at the core region the two approximations coincide [Fig. 7(c)]. Meanwhile, another noticeable aspect of the turbulent motion in such an enclosure is that the turbulence is greater near the cold wall. The reason for this inequality is unstable stratification and two-dimensional heat transfer. So, the effect of molecular viscosity near the floor in the vicinity of the cold wall is to delay (Fig. 8). Since the warm air stays at the upper parts of the room, the turbulent viscosity near the ceiling is high at every section. The ratio of turbulent viscosity to the molecular one decreases towards the core region, and the viscous sub-layer gets thicker near the floor at the sections away from the cold wall. Hot air entering the zone through the upper hole cools at a small distance from the cold wall and causes a disturbance. This situation was illustrated in Figs 5 and 6. Thus, it is concluded that both the secondary flows and the unstable stratification are obtained more clearly by the Daly Harlow approximation.

Also, the flow field in the gap between the double glazed plate and the Trombe wall has been predicted by the Daly Harlow approximation (Fig. 9). The circulation at the down part of the enclosure illustrated in this figure is due to the cooled air coming from the room through the lower opening. The warmed air flow leaving the gap through the upper hole causes sharp velocity changes.

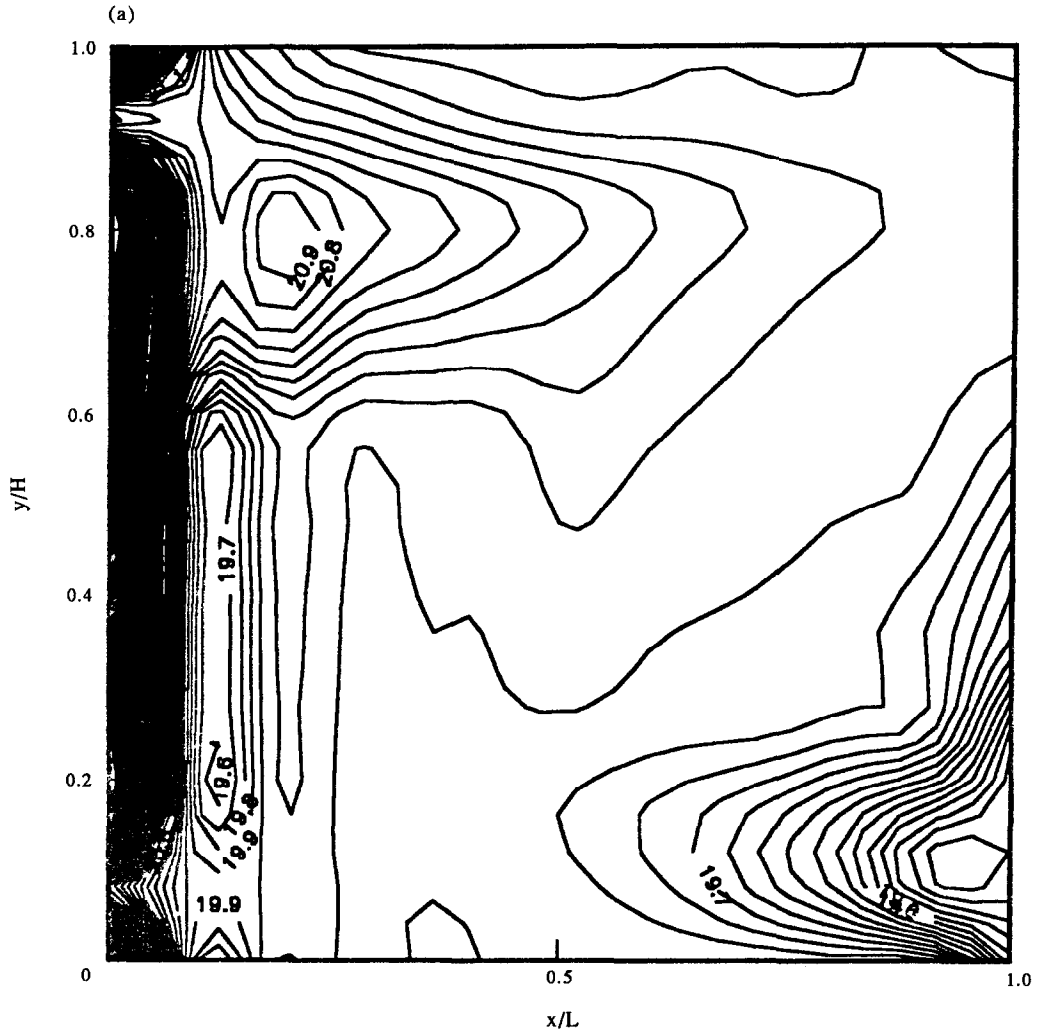

Fig. 6(a)—*caption opposite.*

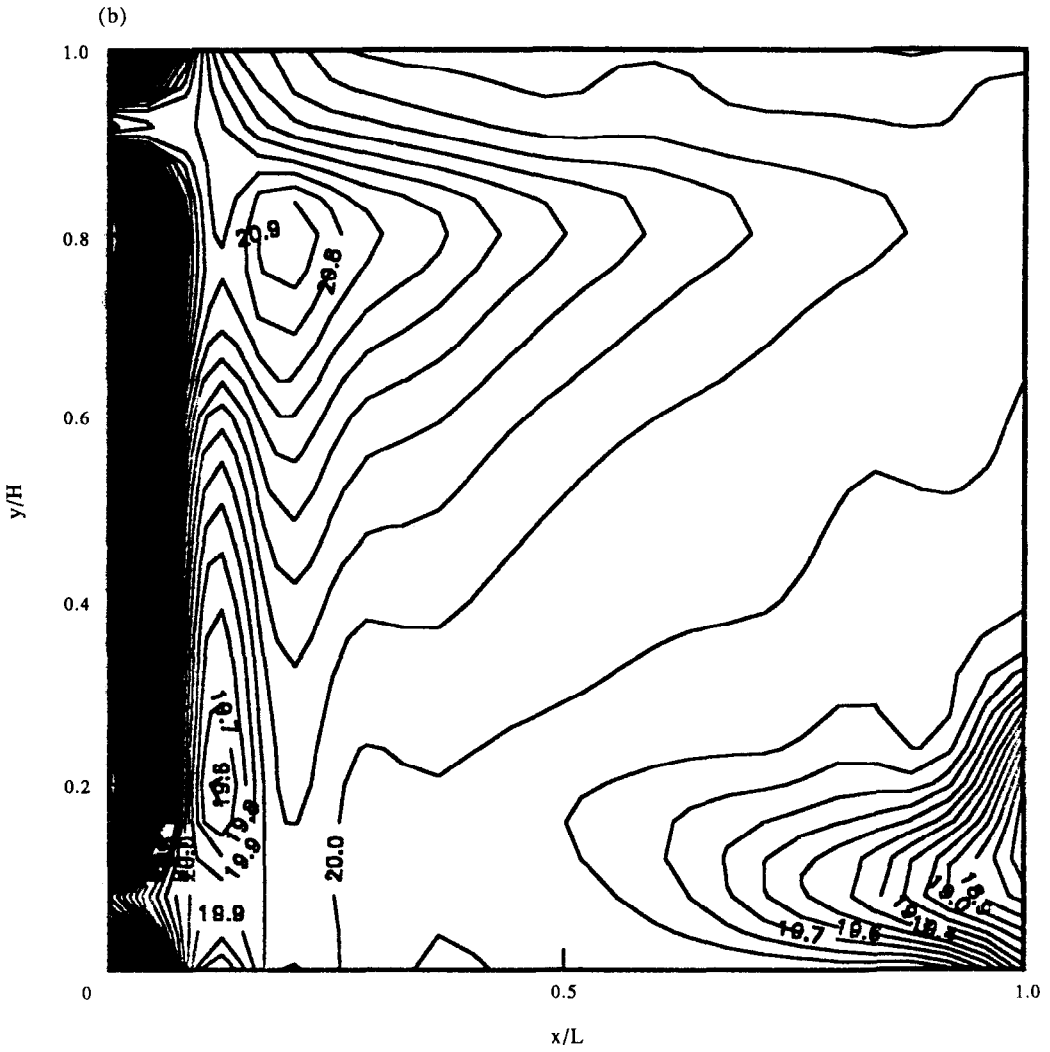

Fig. 6. Temperature contours in the passively heated zone with a Trombe wall: (a) Standard approximation; (b) Daly Harlow approximation.

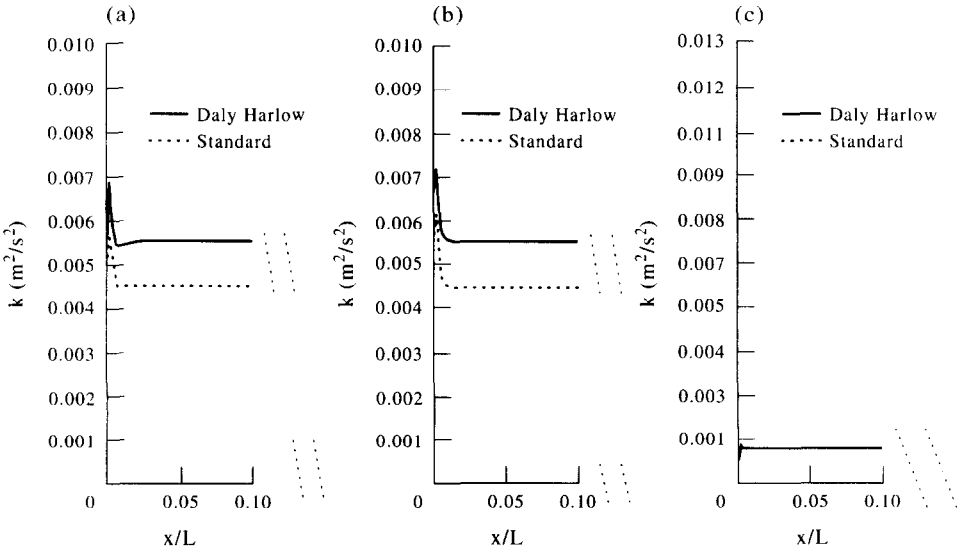

Fig. 7. Change of turbulence kinetic energy in the passively heated zone with a Trombe wall: (a) near the ceiling; (b) near the floor; (c) at the midheight.

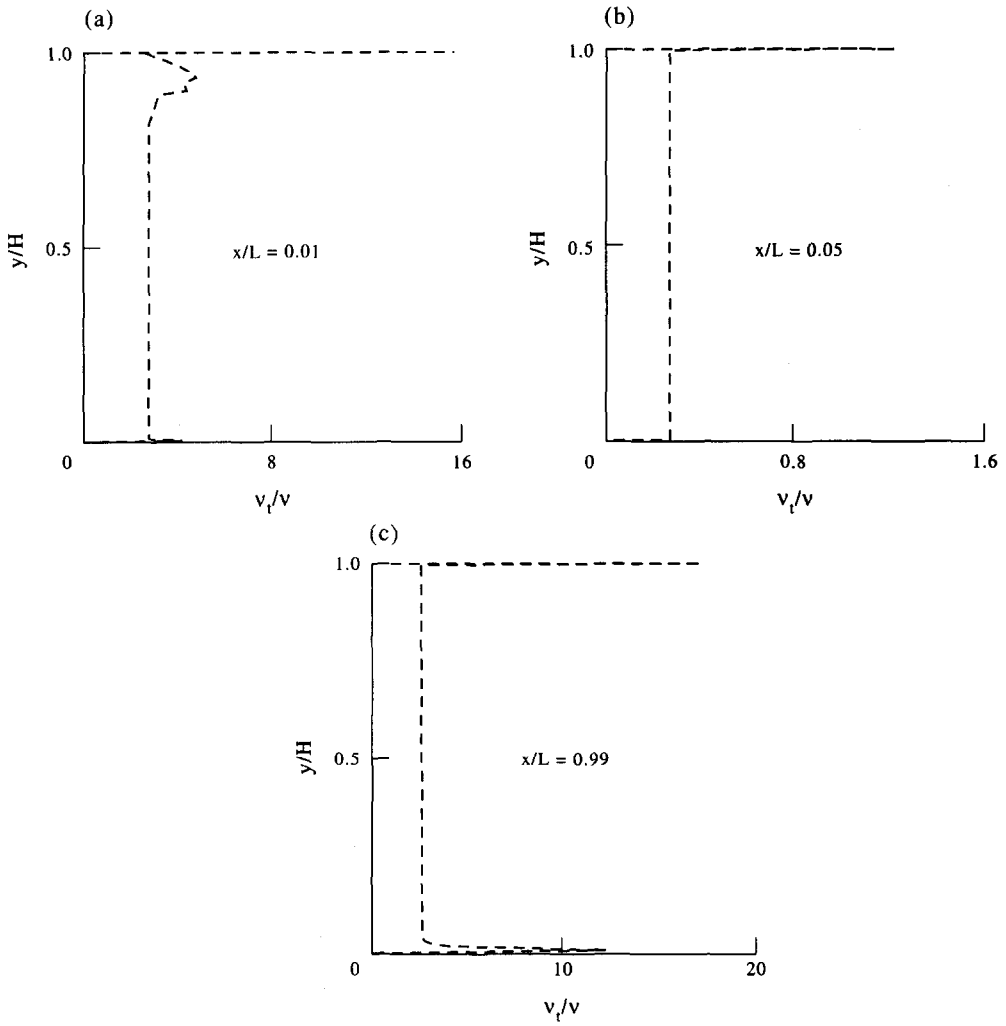

Fig. 8. Change of turbulent viscosity in the passively heated zone with a Trombe wall: (a) near the Trombe wall; (b) at the centre; (c) near the cold wall.

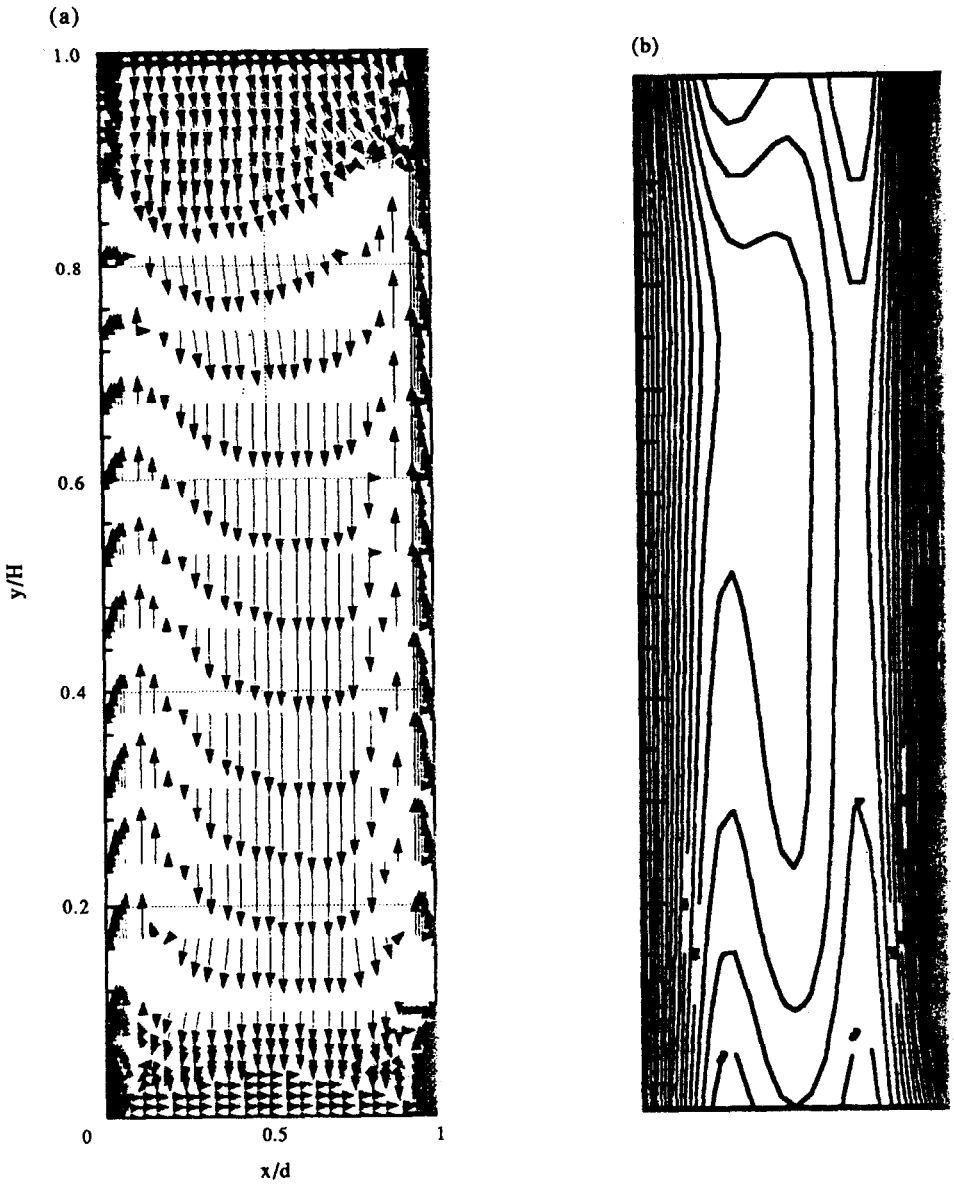

Fig. 9. Flow field between the double glazed plate and the Trombe wall: (a) velocity vectors; (b) temperature contours.

Due to the terms added to the energy equation [equation (15)], the Daly Harlow approximation also supplies a rapid convergence which is hard to obtain in calculation of non-isothermal turbulent flows. However, using this approximation for only the definition of the scalar quantities is not enough. Also, non-isotropy of the vectoral fluctuations should be taken into consideration to obtain more clear representations of the secondary flows, and a hybrid model, including the non-isotropy of the Reynolds stresses in certain parts of the flow domain, should be developed.

REFERENCES

1. A. E. Gill, The boundary layer regime for convection in a rectangular cavity. *J. Fluid Mech.* **26,** 515 (1966).
2. S. Ostrach, Natural convection in enclosures. *Advances Heat Transfer* **8,** 161 (1972).
3. A. Bejan, *Convection Heat Transfer*. Wiley, New York (1984).
4. A. T. Kirkpatrick and A. Bohn, Flow visualization and stratification in high Rayleigh number mixed cavity natural convection. *Nat. Heat Transfer Conf., ASME* 85, HT-38 (1985).
5. C. K. Boardman III, A. Kirkpatrick and R. Anderson, Influence of aperture height and width on interzonal natural convection in a full-scale air-filled enclosure. *Trans. ASME, J. Solar Energy Engng* **111,** 278 (1989).
6. N. Z. Ince and B. E. Launder, On the computation of buoyancy-driven turbulent flows in rectangular enclosures. *Int. J. Heat Fluid Flow* **10,** No. 2 (1989).
7. P. L. Betts and A. A. Dafa'alla, Turbulent buoyant air-flow in a tall rectangular cavity. *Significant Questions in Buoyancy Affected Enclosures or Cavity Flows, HTD-60, ASME Winter Annual Meeting*, p. 83, Anaheim (1986).
8. R. A. W. M. Henkes, F. F. Van der Vlugt and C. J. Hoogendorn, Natural convection in a square cavity calculated with low Reynolds number turbulence models. *Int. J. Heat Mass Transfer* **24,** 377 (1991).
9. M. Behnia, R. Cooper, G. de Vahl Davis, E. de Leonardi, D. Naot, J. A. Reizes and M. Wolfshtein, Turbulent natural convection in a rectangular cavity. *Int. Symp. Computational Fluid Dynamics*, The Univ. of Sydney (1988).
10. P. V. Nielsen, Air flow pattern within buildings. International Energy Agency, Annex 20, Institute for Bygning-teknik, Aalborg Denmark (1990).
11. J. L. Lage and A. Bejan, Efficiency of transient contaminant removal from a slot ventilated enclosure. *Int. J. Heat Mass Transfer* **34,** 2603 (1991).
12. R. Anderson, V. Hassani, A. Kirkpatrick, K. Knapmiller and D. Hittle, Experimental and computational visualization of cold air ceiling jets. *ASHRAE J.* (1991).
13. S. Murakami and S. Kato, Numerical and experimental study on room airflow—3-D predictions using the k-ϵ turbulence model. *Building Environ.* **24,** 85 (1989).
14. S. Murakami, S. Kato and H. Nakagawa, Numerical prediction of horizontal non-isothermal 3-jet in room based on the k-ϵ model. *ASHRAE Trans.* **97,** Part 1 (1991).
15. S. Murakami, S. Kato and H. Nakagawa, Numerical prediction of horizontal non-isothermal 3-D jet in room based on algebraic second moment closure. *ASHRAE Trans.* **98,** Part 1 (1992).
16. J. A. Duffie and W. A. Beckman, *Solar Engng Thermal Processes*, 2nd edn. Wiley, New York (1991).
17. N. Eğrican and S. Uygur, Fluid flow and heat transfer characteristics in single-zone Trombe wall systems. *ISES Solar World Congr.*, Budapest, Hungary (1993).
18. S. Uygur, Natural turbulent convection in passive systems. Ph.D. thesis, Istanbul Technical Univ., Istanbul, Turkey (1993) (in Turkish).
19. Q. Chen, A. Moser and A. Huber, Prediction of turbulent buoyant flow by a low Reynolds number k-ϵ model. *ASHRAE Trans.* **96,** Part 1 (1990).
20. C. V. Patel, W. Rodi and G. Scheurer, Turbulence models for near wall and low Reynolds number flows: a review. *Am. Inst. Aeronautics and Astronautics (AIAA) J.* **23,** 1308 (1986).
21. B. E. Launder, Low Reynolds number turbulence near walls. Report: TFD/86/D, UMIST (1986).
22. R. J. Yang and W. Aung, Equations and coefficients for turbulence modeling. In *Natural Convection* (Edited by S. Kakac) (1986).
23. W. P. Jones and B. E. Launder, The prediction of laminarization with a two equation model of turbulence. *Int. J. Heat Mass Transfer* **15,** 301 (1972).
24. B. E. Launder and D. B. Spalding, The numerical computation of turbulent flows. *Computer Meth. Appl. Mech. Engng* **3,** 269 (1974).
25. B. J. Daly and F. H. Harlow, Transport equations in turbulence. In *Turbulence Transport Modeling*, AIAA Selected Reprint Series, AIAA, New York (1973).
26. S. V. Patankar, *Numerical Heat Transfer and Fluid Flow*. Hemisphere, New York (1980).
27. M. Mbaye and E. Bilgen, Natural convection and conduction in porous wall, solar collector systems without vents. *J. Energy Engng, Trans. ASME* **114,** 40 (1992).

APPENDIX

Modeling the Convective Flow in Porous Trombe Wall

To model the flow inside the Trombe wall, both the brick structure and the orientation of the holes on the wall have been taken into consideration (Fig. A1). Using the criteria in Ref. [3];

$$\mathrm{Re} = \frac{\rho U K'^{1/2}}{\mu} \leqslant 1 \tag{A1}$$

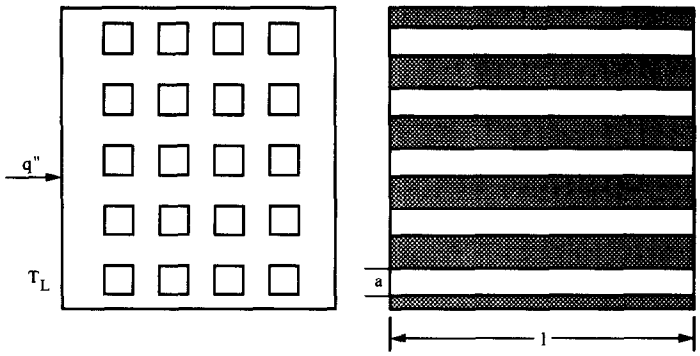

Fig. A1. Brick structure of the Trombe wall.

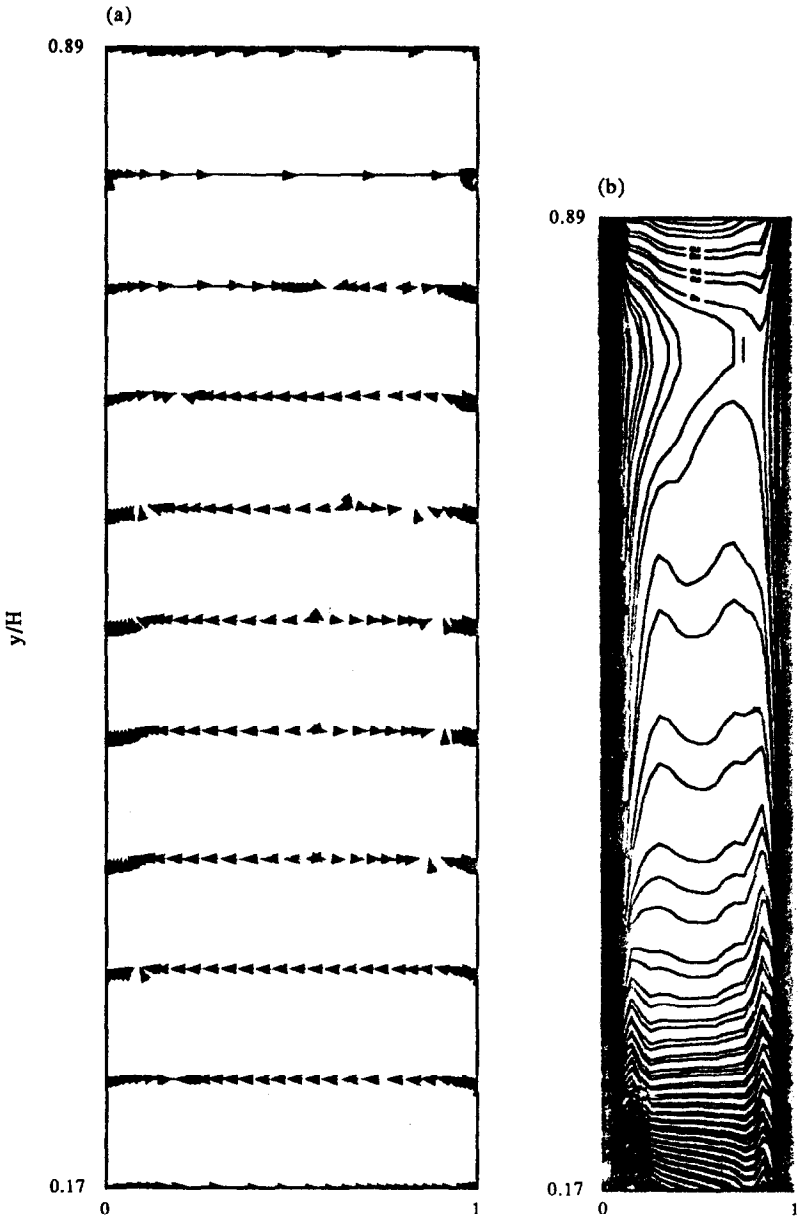

Fig. A2. Flow field inside the Trombe wall between the ventilation holes: (a) velocity vectors; (b) temperature contours.

where U and K' are, respectively, the horizontal velocity in the porous media and permeability, it has been concluded that the flow inside the wall is laminar.

Permeability is defined in terms of porosity as:

$$K' = \frac{a^2\Phi^3}{(1-\Phi)^2}. \tag{A2}$$

Porosity is the sum of the surface porosity, 0.2 for the material of the Trombe wall, and the ratio of the void space to the solid space. Thus:

$$\Phi = \frac{20a^2L}{V_{\text{solid}}} + 0.2. \tag{A3}$$

The terms a and I appearing in equations (A2) and (A3) are the dimensions of the holes on the brick (Fig. A1).

The governing equations of the laminar flow in fluid media have been combined with the Darcy's Law as the following equations [27]:

$$\frac{\partial U}{\partial x} + \frac{\partial V}{\partial y} = 0 \tag{A4}$$

$$\rho U\frac{\partial U}{\partial x} + \rho V\frac{\partial U}{\partial y} = -\frac{\partial P}{\partial x} + \mu'\nabla^2 U - \frac{\mu}{K'}U \tag{A5}$$

$$\rho U\frac{\partial V}{\partial x} + \rho V\frac{\partial V}{\partial y} = -\frac{\partial P}{\partial y} + \mu'\nabla^2 V - \frac{\mu}{K'}V + \rho g\beta(T - T_L) \tag{A6}$$

$$\rho c_p U\frac{\partial T}{\partial x} + \rho c_p V\frac{\partial T}{\partial y} = k\nabla^2 T \tag{A7}$$

where U and V are velocity components in the x and y directions.

The thermal conductivity, k, is calculated with the assumption that the heat is transferred via the fluid and porous media, in series.

The dynamic viscosity, μ', is assumed as equal for the fluid and the porous media [27].

Equations (A4)–(A7) have been solved simultaneously, and the convective flow field inside the Trombe wall has been obtained as illustrated in Fig. A2.